Solar Phys (2012) 279:453–464
DOI 10.1007/s11207-012-0037-2

Hα Line Impact Linear Polarization Observed in the 23 July 2002 Flare with the Large Solar Vacuum Telescope (LSVT)

N.M. Firstova · V.I. Polyakov · A.V. Firstova

Received: 22 September 2011 / Accepted: 14 May 2012 / Published online: 6 June 2012

Abstract We present the results of studying the proton flare 2B/X4.8 on 23 July 2002, observed with the *Large Solar Vacuum Telescope* (LSVT) at the Baikal Astrophysical Observatory in spectropolarimetric mode with high spatial and spectral resolution. We have found some evidence for Hα line impact linear polarization, predominantly during the initial moments of the flare. For the Hα line 606 cuts were made along the dispersion in 53 spectrograms, and a polarization signal was found more or less confidently in 60 cuts (13 spectrograms). Polarization was mainly observed in one of the kernels of the flare. A particular feature of this kernel was that the Hα line was observed to show a reversal in the central part of this kernel, which created a dip in the kernel center in the photometric cut. The size of these dips and the size of the sites with the linear polarization coincide and are equal to 3 – 6 arcsec. The maximum polarization degree in this kernel reached 15 %. The direction of the polarization in the kernel is radial, except for the first two frames, where the direction of the polarization was both radial and tangential. Furthermore, we found an analogy between the effects observed at the chromospheric level in this kernel (polarization and depression in Hα line) and the temporal variation of the HXR sources.

Keywords Solar flare · Spectrograph · Impact polarization

1. Introduction

The relative contribution of the accelerated particle beams to chromospheric heating during solar flares can be estimated by studying the hydrogen line impact linear polarization that arises due to the anisotropic effect of particle beams on the hydrogen atom (Hénoux and Chambe, 1990; Fletcher and Brown, 1995; Vogt, Sahal-Brechot, and Hénoux, 1997; Emslie *et al.*, 2000). The initiator and pioneer of observing the impact polarization in solar flares was J.-C. Hénoux. The linear polarization in flares was revealed using filtergrams covering

N.M. Firstova (✉) · V.I. Polyakov · A.V. Firstova
Institute of Solar-Terrestrial Physics, Siberian Branch, Russian Academy of Sciences, P.O. Box 291, Irkutsk 33, 664033, Russia
e-mail: first@iszf.irk.ru

the entire flare (Vogt and Hénoux 1996, 1999); it was estimated by UV chromospheric lines (Hénoux *et al.*, 1983) and also by using the THEMIS spectral observations (Hénoux *et al.*, 2004; Hénoux and Karlicky, 2003; Xu *et al.*, 2005).

For several years, the Hα line impact linear polarization in flares has been observed with the *Large Solar Vacuum Telescope* (LSVT) at the Baikal Astrophysical Observatory, affiliated with the Russian Institute of Solar and Terrestrial Physics (Skomorovsky and Firstova, 1996). As a result of this research, the impact polarization signature in some flares has been obtained (Firstova and Boulatov, 1996; Firstova *et al.*, 1997; Firstova and Kashapova, 2002). Thus, various researchers at different telescopes have obtained some evidence for the existence of linear polarization in solar flares; the evidence is, however, scarce. Furthermore, Bianda *et al.* (2005) did not obtain any clear linear polarization signature in high-sensitivity observations of 30 flares.

On 23 July 2002, a major 2B/X4.8 flare occurred at S13E72 on the solar disk. According to *Solar Geophysical Data*, it began at 00:15 UT, reached maximum at 00:35 UT and ended after 02:00 UT. The LSVT enabled us to make observations of the flare in the spectropolarimetric mode with high spatial, temporal and spectral resolution. Pre-processing of the spectrograms showed that it had a linear polarization signature (at least, at flare onset) (Firstova, Xu, and Fang, 2003). Half of 247 spectrograms of this flare were then processed in detail, and the results of this were published in Firstova, Polyakov, and Firstova (2008). In that paper, we presented some evidence for a very high degree of linear polarization and we showed the distribution of the Stokes parameters across the flare ribbons.

Unfortunately, the data analyzed and presented in that paper had a systematic data reduction error, which made all the results flawed. It turned out that the distance between the positions of the upper and lower spectral stripes (ordinary and extraordinary rays) used in that analysis was erroneous by two pixels. Despite the fact that two pixels correspond to 0.34 arcsec in a solar image on the spectrograph slit, and the real resolution during the flare observation was 1 – 1.5 arcsec, such an error at high intensity gradients observed during this flare led to the occurrence of a false polarization signal. In this paper, we re-analyse this data, since the observations obtained in the spectropolarimetric mode of this interesting solar flare are adequate and comprehensive, and they should not be abandoned.

Section 2 presents a brief description of the equipment and technique for spectropolarimetric observations of flares. In Section 3, we describe the study of linear polarization in the flare, using cuts along the dispersion. In Section 4 we discuss the results, and in Section 5 the conclusions are given.

2. Spectropolarimetric Method to Observe Flares with LSVT

Let us briefly describe the observation conditions for this flare. The LSVT theoretical spatial resolution is 0.3 arcsec; depending on atmospheric conditions this value ranges within 1 – 3 arcsec *de facto*. Spectropolarimetric observations were carried out in the Hα line with a Princeton Instruments CCD camera. One CCD camera pixel corresponds to 0.17 arcsec and 0.0197 Å.

The spectrograph has a mirror slit. When observing this flare, tracking its evolution was done visually using the solar image reflected from the mirror slit through a 0.5 Å passband birefringent filter in the Hα line.

A rhomboid was placed behind the spectrograph slit. It separated the ordinary rays from the extraordinary ones and allowed us to record the solar spectrum simultaneously in two mutually orthogonal polarizations.

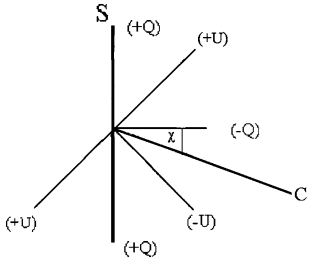

Figure 1 Determining the Stokes parameters of planes in the LSVT spectrograph system. S is the spectrograph slit position. C is the direction towards the center of the solar disk.

During observations, we placed the most interesting (usually the brightest) flare kernels on the spectrograph slit and made several exposures alternately at two positions of the phase half-wave plate (0° and 22.5°). At the first position of the plate, we determined the Stokes parameter Q. The radiation polarized along the spectrograph slit was recorded in the upper spectral stripe ($I_1 = I + S$), whereas the perpendicular one (along the dispersion) was recorded in the lower spectral stripe ($I_2 = I - S$). At the second position of the phase plate, we recorded the radiation polarized at $\pm 45°$ angles in the upper and lower spectral stripes. This allowed us to determine the Stokes parameter U. The time interval between the spectrograms (odd for determining Q and even for determining U) was usually 6 – 10 s.

Unfortunately, the very first spectrograms (up to 20 frames) were obtained without $\lambda/2$ plates, *i.e.* only the Stokes parameter Q is available.

Figure 1 illustrates the position of the spectrograph slit S and the Stokes parameters relative to the direction of the solar disk center. $(+Q)$ or $(+U$, when adding $\lambda/2$ plates) corresponds to the upper spectral stripe I_1 in Figure 1, while $(-Q)$ or $(-U)$ corresponds to I_2.

As Figure 1 illustrates, during the observation of the flare, the angles between the direction of the solar disk center and the $(-Q)$ and $(-U)$ axes are approximately equal. Besides, if the linear polarization coincides with the projection of the vertically incident beam of particles, the polarization direction is radial. The radial direction in Figure 1 is determined by negative values $-Q$ and $-U$. However, usually the polarization radial direction is related to the positive values of the Stokes parameters, whereas the perpendicular direction is related to negative ones. That is why we reversed the signs for the Stokes parameters derived from the observations. Note that the radial direction is observed at small values of the particle beam energy, whereas the polarization perpendicular to this direction (tangential) is observed at high values of the particle energy (Hénoux, 1991).

To minimize the instrumental polarization, the line intensity was normalized to the continuum in each stripe. This procedure almost completely excludes any influence of the instrumental polarization on the Stokes parameter I, but interpenetration of Q and U distorts them. False signals for Q/I and U/I do not exceed 2 % (see the appendix in Firstova, Polyakov, and Firstova, 2008).

In this paper, we made the photometric cuts along the spectrograph slit averaged over seven pixels (0.059 Å) in the Hα line center $I^{\mathrm{H}\alpha}$ and in the remote line wing I^{c} in order to check the accuracy of the distance between the two spectral stripes (Figure 2).

To use our method for minimizing the instrumental polarization, the intensity in the Hα line was normalized to the continuum intensity in each of the spectral stripes:

$$I_1 = I_1^{\mathrm{H}\alpha}/I_1^{\mathrm{c}}, \qquad I_2 = I_2^{\mathrm{H}\alpha}/I_2^{\mathrm{c}}. \tag{1}$$

Figure 3 presents the example of the normalization and superposition of solar features located on two spectral stripes (I_1 and I_2), shown in Figure 2.

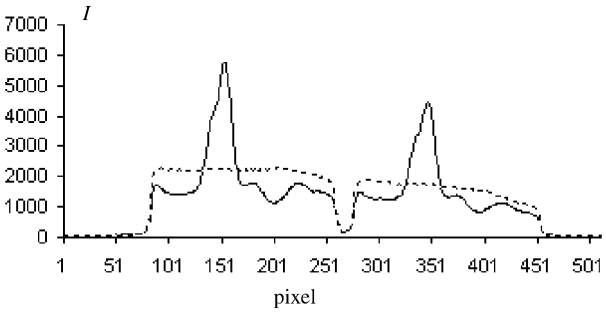

Figure 2 Intensity distributions along the spectrograph slit in the Hα line center (solid line) and in the Hα line's remote wing (dashed line) in two spectral stripes.

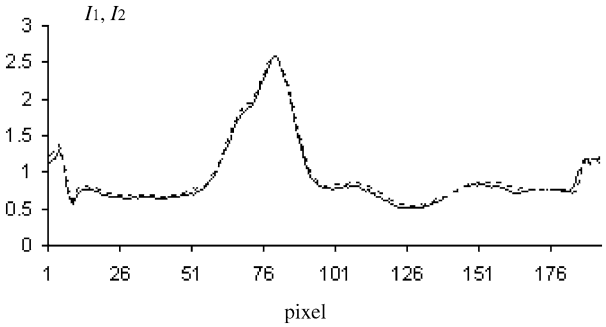

Figure 3 Intensity distributions I_1 (solid line) and I_2 (dashed line) along the spectrograph slit.

At such a better superposition, the distance between the spectral stripes was 193 pixels, while in Firstova, Polyakov, and Firstova (2008) we considered this distance to be equal to 195 pixels. This had led to the false Stokes parameters Q/I and U/I.

3. Determining Stokes Parameters

We made the cuts along the dispersion similarly to how it had been done in Firstova, Polyakov, and Firstova (2008), however, this time the distance between the spectrum stripes used in the analysis was the correct 193 pixels. In each frame of both spectra, 10 – 12 cuts with a 5-pixel (0.85-arcsec) step were made, and averaging along the slit was produced also over five pixels.

Spectrograms were processed using the IDL software. The line intensity was normalized to the continuum intensity in each stripe. For each spectral cut, the Stokes parameters were determined by

$$I = \frac{I_{1\lambda}/I_{1c} + I_{2\lambda}/I_{2c}}{2}, \tag{2}$$

$$Q/I\,(U/I) = \frac{I_{1\lambda}/I_{1c} - I_{2\lambda}/I_{2c}}{I_{1\lambda}/I_{1c} + I_{2\lambda}/I_{2c}}, \tag{3}$$

where $I_{1\lambda}$ and $I_{2\lambda}$ are the Hα line intensity in the upper and lower stripes of a spectrum, and I_{1c} and I_{2c} are the intensities of the remote line wing.

Figure 4 shows two examples of the values $I_{1\lambda}/I_{1c}$, $I_{2\lambda}/I_{2c}$ and also Q/I along the dispersion in two flare kernels received after processing.

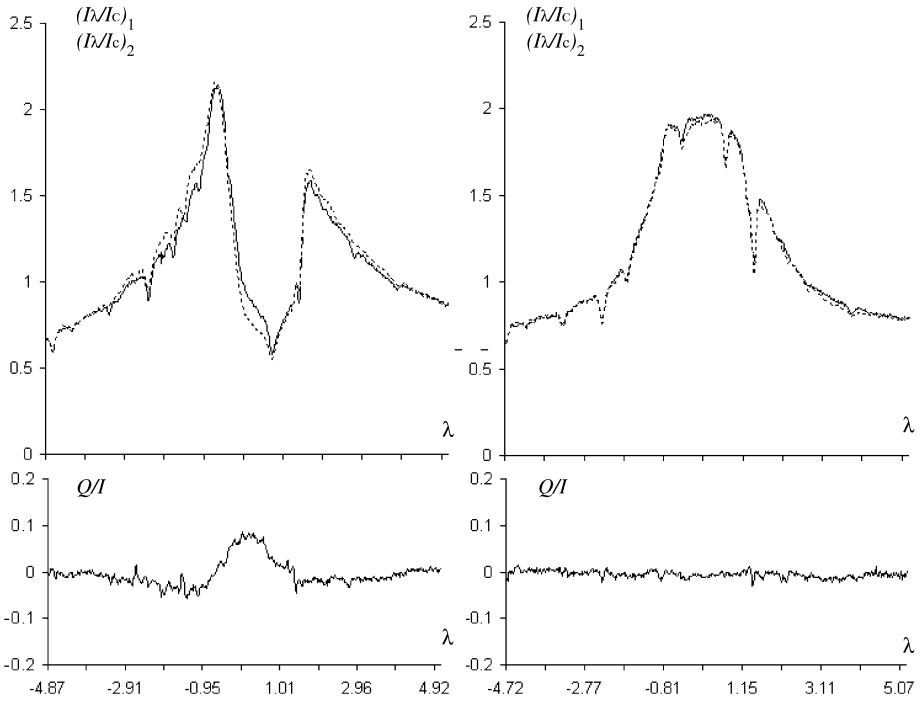

Figure 4 Top: values of $I_{1\lambda}/I_{1c}$ (solid line) and $I_{2\lambda}/I_{2c}$ (dashed line) along the dispersion in two flare kernels, one with ≈ 8 % polarization (left) and another with no polarization signal (right). Bottom: the Stokes parameter Q/I.

The right-hand figure illustrates the absence of the polarization signal in the given flare kernel, while in the left-hand figure we see that the Stokes parameter Q/I reaches 8 %.

The first spectrograms during 1 m 50 s were obtained without a half-wave plate, *i.e.* we could define only the Stokes parameter Q. In these first spectrograms, two flare kernels were recorded, and after processing it was revealed that the linear polarization signature was found only in one of them. It is this kernel where the Hα line has a strong central reversal.

Due to this, we will consider the first 12 frames, and show the first two frames in Figure 5. In the upper panels of the figure, we show the regions of the spectrum at 0:32:09 and 0:32:20 UT (only one spectral stripe ($I + S$)). Further, we give the Q/I profiles along the dispersion for the kernel with the central reversal and for the emission kernel as obtained by several cuts. Besides, in this figure the results can be found of the photometric cuts along the slit: the intensity of the Hα line center, the wing intensity at ~ 1 Å of the Hα line center and the Q/I values.

As can be seen, nonzero values for the Stokes parameters are observed only in the kernel with the central reversal. Besides, the photometric cut plot shows that the Hα line central reversal appears inside the kernel but not on its periphery. We observed neither central reversal nor polarization in the bottom kernel.

Figure 6 presents plots similar to those at the bottom of Figure 5 for all the remaining spectrograms obtained within the first minutes of observation.

The central reversal in the Hα line should look as a dip in the kernel in a photometric cut. We can see these dips in some cuts in Figure 6. The divergence between different photometric cuts in Figure 6 is caused, obviously, by the solar image displacement due to atmospheric

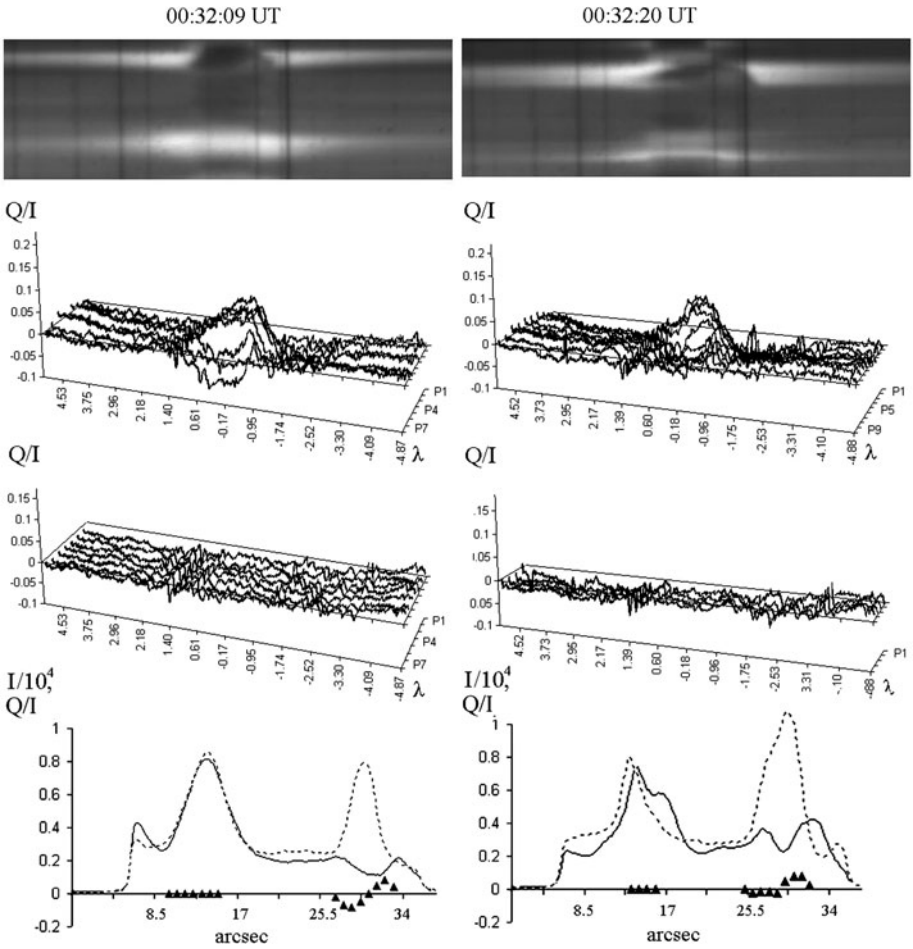

Figure 5 Top: the spectrum in the Hα region at 0:32:09 and 0:32:20 UT. Middle: Q/I profiles along the dispersion for two kernels. Bottom: the solid line denotes the distribution of the Hα line center intensity, the dashed line shows the wing intensity distribution, and triangles present the behavior of the value of Q/I along the slit.

seeing effects. Owing to variable seeing, the depression in the kernel and the polarization signal disappear, and then appear again.

Since the first two spectrograms appeared to be the most interesting in terms of linear polarization, they were reprocessed. In this case, we made three-pixel step (0.5-arcsec) cuts along the dispersion, also averaging the intensity over three pixels. Figure 7 shows the Q/I parameter spatial distribution. Besides, using the slit position relative to the direction of the solar disk center (Figure 1), we can calculate an approximate value of the polarization degree from the Q/I parameter observed:

$$P = \frac{Q/I}{\cos 2\chi} \tag{4}$$

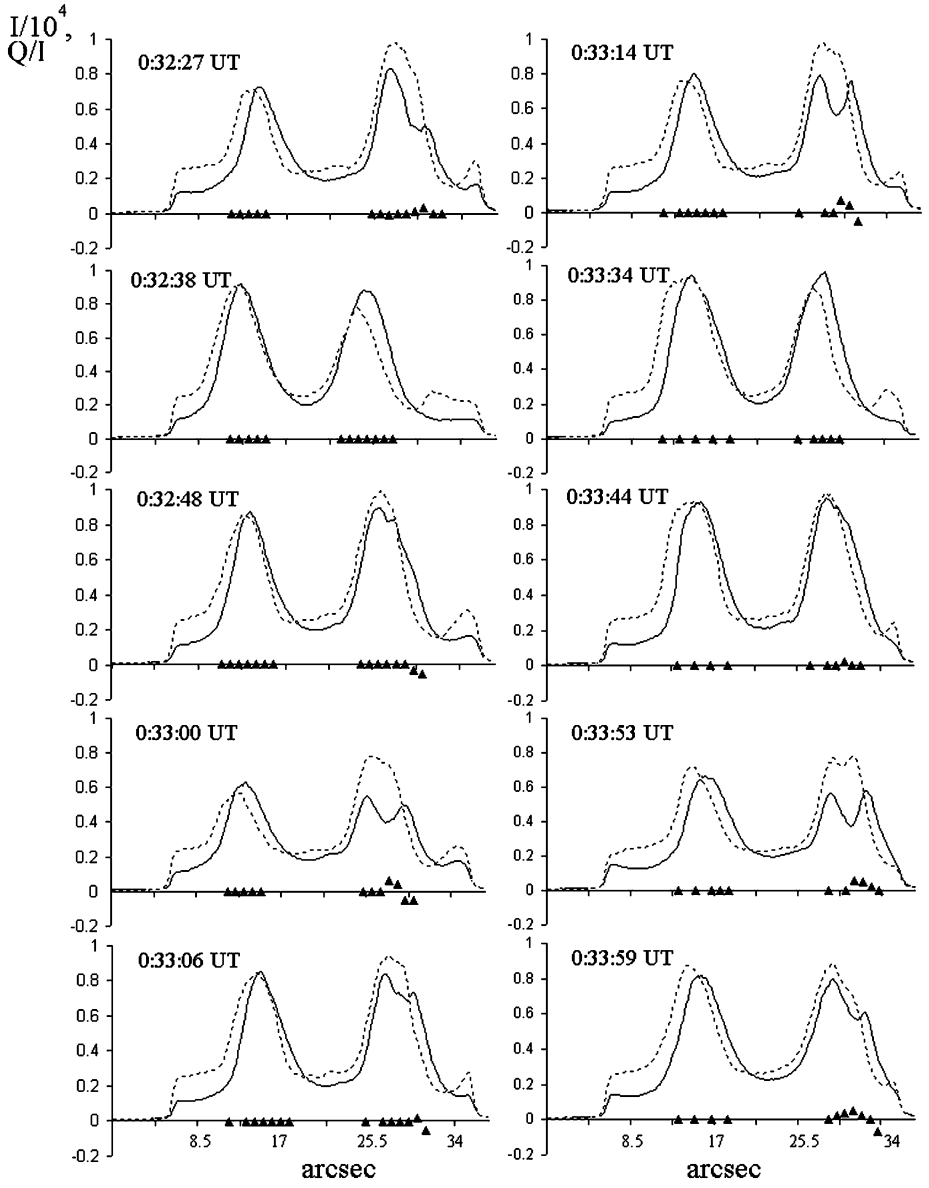

Figure 6 Photometric cuts along the slit: the solid line denotes the Hα line center intensity; the dashed line shows the wing intensity; triangles present the values of Q/I along the slit.

or, on the assumption that $Q/I \approx U/I$:

$$P = \sqrt{(Q/I)^2 + (U/I)^2} \approx \sqrt{2}Q/I. \tag{5}$$

Figure 7 also shows the spatial distribution of the polarization degree P calculated by Equations (4) and (5) for the first two spectrograms.

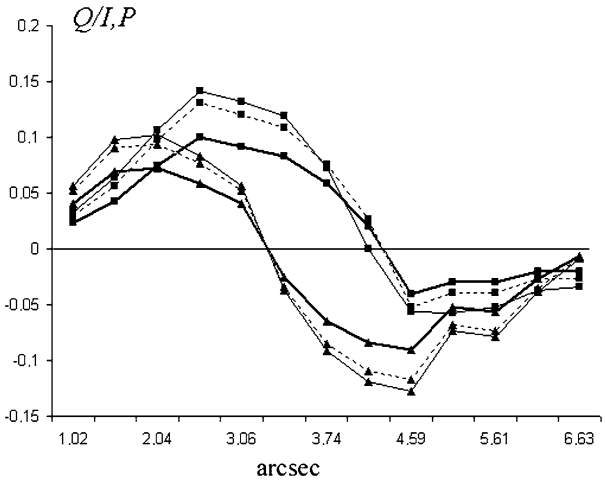

Figure 7 The Q/I distribution (solid heavy line) and P polarization degree (solid line) determined by Equation (4) and dashed line by Equation (5) along the spectrograph slit. Diamonds show the Q/I and P distribution for 0:32:09 UT, triangles present the same for 0:32:20 UT.

The linear polarization degree in Figure 7 (up to 15 % in one of the cuts) is the maximum polarization degree obtained during the first minutes of observation.

Furthermore, we obtained some more spectrograms where there were also signatures of the linear polarization. Like for the first frames (Figures 5 and 6), the polarization appeared in the kernels where the Hα line had the central reversal. However, in some spectrograms, the presence of the central reversal was not accompanied by a polarization signal. The latter occurred when the dip in the Hα line center was on the periphery, not in the kernel center.

In Figure 8 we present two spectrograms obtained with $\lambda/2$ phase plate rotated through 22.5° relative to the spectrograph slit; *i.e.*, in these spectrograms the Stokes parameter U/I was recorded. Like in Figure 5, only one stripe of the spectrum $(S+I)$ is shown here. Below, we present one cut along the dispersion for each of these spectrograms. Values $I_{1\lambda}/I_{1c}$ and $I_{2\lambda}/I_{2c}$ as well as U/I are given for each cut.

At 0:39:24 UT, two flare kernels were recorded. In the lower kernel, there is no polarization signal. In the upper kernel, there is a dip inside the kernel. This dip is not distinct enough since the red-wing intensity falls abruptly. Nevertheless, a polarization signal in the line center is observed, and U/I reaches 7 % in this kernel. In the right spectrogram, one can see an example of a kernel with the Hα line central reversal that is located on the kernel periphery. Ten cuts were made in this spectrogram, and in all of these cuts $U/I = 0$. In the same flare kernel recorded at 0:40:45 UT, without $\lambda/2$ plate, we have $Q/I = 0$, too.

4. Discussing the Observational Data

We processed 53 spectrograms in total and made 606 cuts along the dispersion. Signatures of the linear polarization were found in a fraction of spectrograms only. Therefore, we decided to present all the data with confidently obtained nonzero values of the Stokes parameters in the table. If there was only one cut with values Q/I $(U/I) = 0.02-0.03$ in the spectrogram, we did not include such a cut in Table 1 since from the definition the error is $\Delta Q/I$ $(\Delta U/I) \approx 0.02$. In Table 1, also the dip characteristics in the flare kernel are presented.

Column 1 shows the frame numbers. In Column 3, we present the ratio K of the number of nonzero-value cuts of the Stokes parameter to the full number of cuts made in the

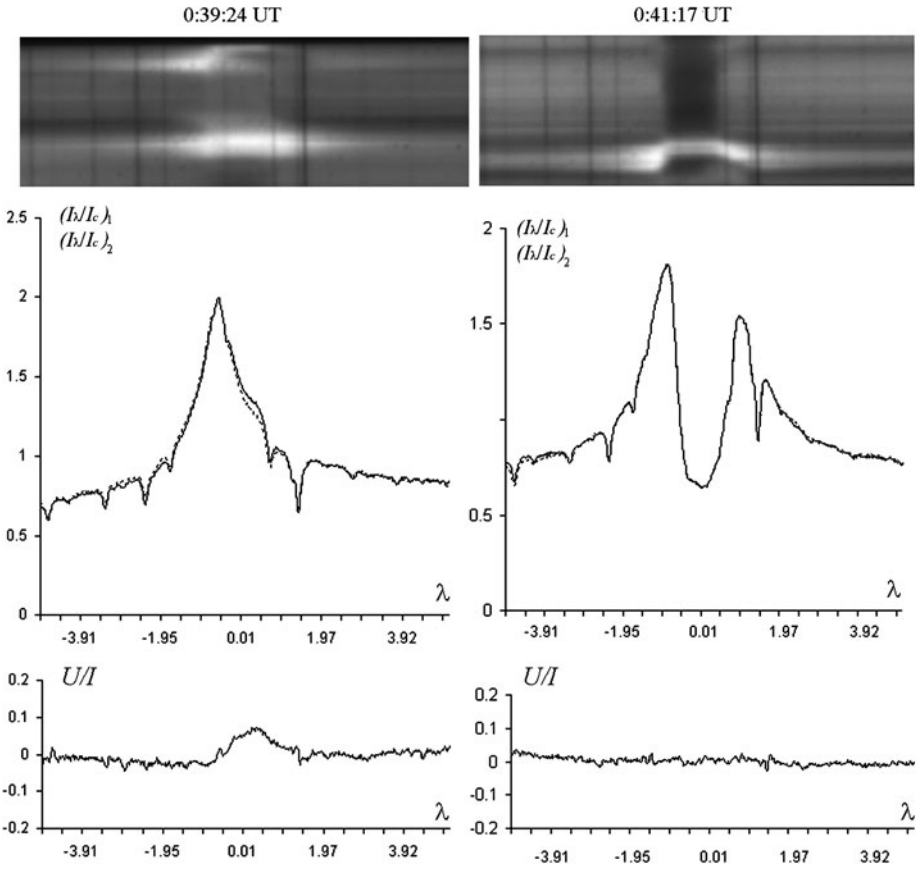

Figure 8 Two spectrograms obtained to determine U/I. Middle: the $I_{1\lambda}/I_{1c}$ distribution (solid line) and $I_{2\lambda}/I_{2c}$ (dashed line) along the dispersion in two flare kernels. Bottom: the distribution of the Stokes parameter U/I.

given spectrogram. In Column 4 the maximum values of Q/I and U/I are given in the given spectrogram (both positive and negative). Column 5 shows the minimum relation (on several cuts in the given spectrogram) of the center line intensity to the blue wing intensity $(I_0/I_w)_{min}$ at 1 Å from the Hα center. Column 6 presents the ratios I_{min}/I_{max} of the intensity in the dip to the maximum intensity on both sides of the given kernel along the spectrograph slit. Column 7 exhibits the size $D(Q/I(U/I))$ of the area with the nonzero values of the Stokes parameters. This size was determined through multiplying the number of cuts with the nonzero values of Q/I and (U/I) by the step along the spectrograph slit. For the first two spectrograms the step made was 0.51 arcsec; the other cuts were made at 0.85 arcsec. The last column gives size D for the area occupied by the dip. This size was determined as the distance between the brightest points on both sides of the kernel from the dip.

Although the flare image moved along the spectrograph slit, this motion was insignificant, at least, up to Frame 44. Careful checking showed that these spectrograms were very similar. Therefore, the observation recorded in these frames were obtained of the same region of the flare. In these cases, the slit crossed two ribbons of the flare which one can see in Figures 5 and 8. In Frames 36, 37 and 43, as well as in Frames 8 and 9, the dip was

Table 1 Characteristics of the Stokes parameters and of the dip (central line reversal) in flare kernels.

Frame number	Time (UT)	K	Q/I (U/I)	$(I_0/I_w)_{min}$	I_{min}/I_{max}	$D(Q/I$ (U/I))	D of dip
8	0:32:09	12/15	$(Q/I)_{max} = 0.05$ (-0.08)	0.14	0,51; 0.53	$6.1''$	$6.0''$
9	0:32:20	11/14	$(Q/I)_{max} = 0.09$ (-0.04)	0.23	0,69; 0.54	$5.6''$	$3.4''$
10	0:32:27	7/15	$(Q/I)_{max} = 0.03$	0.48	0,55; 0.97	$6.0''$	$3.6''$
13	0:33:00	4/12	$(Q/I)_{max} = 0.06$	0.52	0,71; 0.80	$3.4''$	$3.9''$
15	0:33:14	3/10	$(Q/I)_{max} = 0.07$	0.57	0,68; 0.69	$2.6''$	$3.1''$
18	0:33:53	3/11	$(Q/I)_{max} = 0.06$	0.49	0,66; 0.60	$2.6''$	$3.6''$
19	0:33:59	4/11	$(Q/I)_{max} = 0.05$	0.65	0,74; 0.97	$3.4''$	$3.1''$
30	0:36:49	2/16	$(Q/I)_{max} = -0.04$	0.47	0.22	$1.7''$	
36	0:38:13	4/7	$(Q/I)_{max} = 0.12$	0.33	0,72; 0.69	$3.4''$	$4.1''$
43	0:39:24	4/17	$(U/I)_{max} = 0.07$	0.47	0.75; 0.71	$3.4''$	$2.9''$
63	0:44:22	2/9	$(U/I)_{max} = 0.04$	0.52	0.27	$1.7''$	
64	0:44:28	2/11	$(Q/I)_{max} = 0.03$	0.47	0.28	$1.7''$	
65	0:44:36	2/11	$(U/I)_{max} = 0.04$	0.42	0.30	$1.7''$	

observed only in the top kernel. As seen from Table 1, Q/I reached its maximum value (12 %) in Frame 36, and U/I reached its maximum (7 %) in Frame 43. In Frame 37, the dip was located at the very end of the spectrogram, where we do not trust the polarization measurements. In other frames (including Frame 30), there was no depression in the top kernel, which can be caused both by the flare's own shift and by atmospheric seeing effects.

In Spectrograms 30, 63 – 65, the Hα line central reversal was observed not inside the kernel, but on its periphery. Those were the cases similar to the ones presented in the right panel of Figure 8. The confidence level of the Stokes parameters is low, as their values are close to the measurement error.

Thus, one is under the impression that the polarization was confidently observed only in one kernel for 7 minutes (0:32:09 through 0:39:24 UT), and only when the dip (central reversal in the Hα line) appeared inside the flare kernel, but not on its periphery. As per Table 1, 52 cuts of 60 with nonzero values for the Stokes parameters refer to this kernel.

The last two columns in the table show good agreement between the size of the sites with nonzero values for the Stokes parameters and the size of the dips in the kernel. These sizes are also in good agreement with the sizes of the hard X-ray radiation sources in this flare (Krucker, Hurford, and Lin, 2003). This suggests some role for the electron beams in the effects that we observed. Besides, according to Brown, Canfield, and Robertson (1978), Canfield (1974), Fang, Hénoux, and Gan (1993), Ricchiazzi and Canfield (1983), and Canfield, Gunkler, and Ricchiazzi (1984), accelerated electron beams bombarding the chromosphere during a flare lead to a deep central reversal in the Hα line. On the other hand, using the temperature distributions F1 and F2 of the flare's semiempirical models (Machado *et al.*, 1980) and taking into account the impact of proton beams, Hénoux, Fang, and Gan (1993) concluded that in the Hα line there was no central reversal. Assuming that both the observable polarization and the observable central reversal can be caused by electron beams, we compared the time evolution of the X-ray sources for this flare after the RHESSI data (Krucker, Hurford, and Lin, 2003) and the temporal distribution of the Stokes parameters in Figure 9.

Although we observed actually one region of the flare until ≈00:40, we seldom got into a very narrow site of the kernel with the dip that usually was 3 – 4 arcsec wide. When that occurred, we observed, confidently enough, the values of Q/I over the time interval

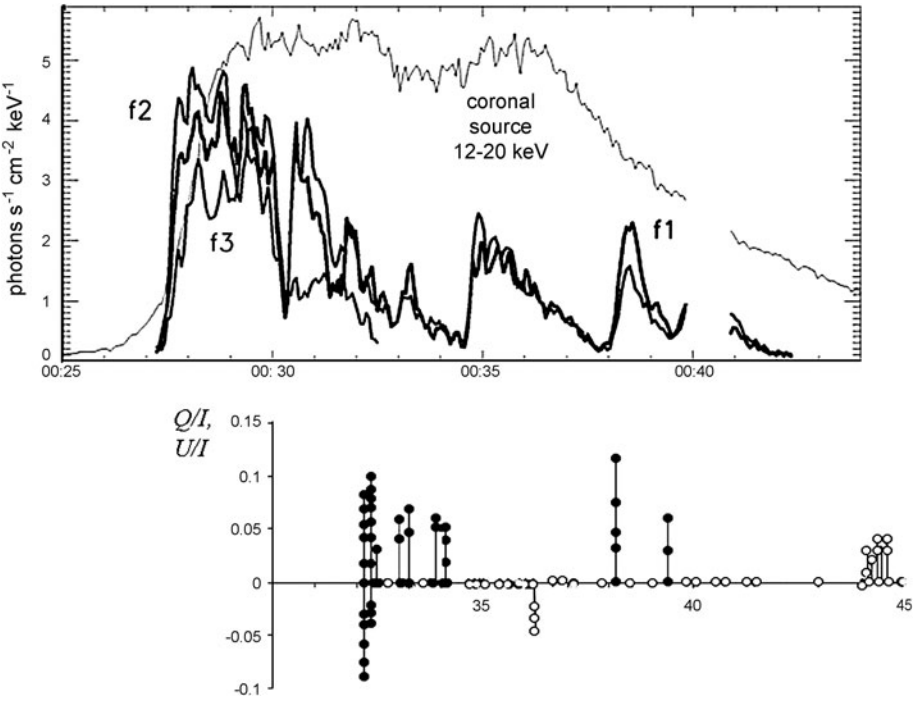

Figure 9 Temperature variation of the HXR sources after RHESSI data for this flare and the distribution of the Stokes parameters Q/I (U/I) at the same time. Black circles show values of Q/I (U/I) in the kernel with a dip.

of 00:32 through 00:34 UT and the two values of Q/I and U/I over the period of 00:37 through 00:40 UT (Figure 9). Thus, at least, the linear polarization in the kernel with a dip was observed during two of the three X-ray peaks. We assume that one of the three X-ray sources is associated with that kernel where we observed a nonzero polarization. Therefore, we conclude that the polarization in the kernel was caused by the residual electrons that penetrated into the chromosphere during the flare.

5. Conclusions

The aim of this study was to find out whether there is a linear polarization in solar flares, because in the research community one does not have an unambiguous opinion about it. Besides, we had to check the existence of polarization in the 23 July 2002 flare, since we had made a mistake when processing the spectrograms in our previous analysis (Firstova, Polyakov, and Firstova, 2008).

Using the detailed analysis of the spectropolarimetric observations of the flare in the line, we arrived at the following conclusions:

i) In the bulk of the spectrograms for this flare, we found no real proof of the existence of linear polarization. Of 606 cuts made along the dispersion in 53 spectrograms, a polarization signal was revealed, more or less confidently, at 60 cuts (13 spectrograms). Linear polarization usually appears in flare regions with Hα line central reversal.

ii) We observed linear polarization most confidently in one of the flare kernels that appeared on the spectrograph slit at the very beginning of the observation and then would last for seven minutes. Of 60 cases of nonzero values for the Stokes parameters, 52 refer to this kernel, and the value of the polarization degree maximum is 15 %. At the very beginning of the observation (0:32:09 UT and 0:32:20 UT), the high-degree polarization had both radial ($Q/I = +9$ %) and tangential ($Q/I = -8$ %) directions. In other cases, the polarization had a radial direction. The polarization existed in small-scale (3 – 6-arcsec) sites. Simultaneously, at these sites the Hα line had central reversal, which formed a 3 – 6-arcsec dip in the center of the kernel.

iii) We suppose that the electron beams bombarding the chromosphere during the flare caused the observed linear polarization.

iv) As per conclusions i) – ii), it seems to be difficult enough to detect linear polarization in flares, and it is easier to speak about the absence of this effect rather than about its presence. We think that the telescope's spatial resolution is important in the success of detection, since the size of the flare regions showing polarization is very small. Besides, recording a flare's impulsive phase is of great importance, as linear polarization seems to be present mainly then.

References

Bianda, M., Benz, A.O., Stenflo, J.O., Kuveler, G., Ramelli, R.: 2005, *Astron. Astrophys.* **434**, 1183.
Brown, J.C., Canfield, R.C., Robertson, M.N.: 1978, *Solar Phys.* **57**, 399.
Canfield, R.C.: 1974, *Solar Phys.* **34**, 339.
Canfield, R.C., Gunkler, T.A., Ricchiazzi, P.J.: 1984, *Astrophys. J.* **282**, 296.
Emslie, A.G., Miller, J.A., Vogt, E., Hénoux, J.-C., Sahal-Brechot, S.: 2000, *Astrophys. J.* **542**, 513.
Fang, C., Hénoux, J.C., Gan, W.Q.: 1993, *Astron. Astrophys.* **274**, 917.
Firstova, N.M., Boulatov, A.V.: 1996, *Solar Phys.* **164**, 361.
Firstova, N.M., Kashapova, L.K.: 2002, *Astron. Astrophys.* **388**, L17.
Firstova, N.M., Polyakov, V.I., Firstova, A.V.: 2008, *Solar Phys.* **249**, 53.
Firstova, N.M., Xu, Z., Fang, C.: 2003, *Astrophys. J. Lett.* **595**, L131.
Firstova, N.M., Hénoux, J.-C., Kazantsev, S.A., Bulatov, A.V.: 1997, *Solar Phys.* **171**, 123.
Fletcher, L., Brown, J.C.: 1995, *Astron. Astrophys.* **294**, 260.
Hénoux, J.-C.: 1991, In: *Proceedings of 11th National Solar Observatory Janame Peak Workshop*, 285.
Hénoux, J.-C., Chambe, G.: 1990, *J. Quant. Spectrosc. Radiat. Transf.* **44**(N1), 193.
Hénoux, J.-C., Karlicky, M.: 2003, *Astron. Astrophys.* **407**, 1103.
Hénoux, J.-C., Fang, C., Gan, W.Q.: 1993, *Astron. Astrophys.* **274**, 923.
Hénoux, J.-C., Chambe, G., Semel, M., Sahal, S., Wootgate, B., Shine, D., Beckers, J., Machado, M.: 1983, *Astrophys. J.* **265**, 1066.
Hénoux, J.-C., Vogt, E., Chambe, G., Briand, C.: 2004, *Nuovo Cimento* **25C**(5 – 6), 729.
Krucker, S., Hurford, G.J., Lin, R.P.: 2003, *Astrophys. J. Lett.* **595**, L103.
Machado, M.E., Avrett, E.H., Vernazza, J.E., Noyes, R.W.: 1980, *Astrophys. J.* **242**, 336.
Ricchiazzi, P.J., Canfield, R.C.: 1983, *Astrophys. J.* **272**, 739.
Skomorovsky, V.I., Firstova, N.M.: 1996, *Solar Phys.* **163**, 209.
Vogt, E., Hénoux, J.-C.: 1996, *Solar Phys.* **164**, 345.
Vogt, E., Hénoux, J.-C.: 1999, *Astron. Astrophys.* **349**, 283.
Vogt, E., Sahal-Brechot, S., Hénoux, J.-C.: 1997, *Astron. Astrophys.* **324**, 1121.
Xu, Z., Hénoux, J.-C., Chambe, G., Karlicky, M., Fang, C.: 2005, *Astrophys. J.* **631**, 618.